ACS Macro Letters

pubs.acs.org/macroletters Letter

Thiol- and Disulfide-Functionalized Polycyclooctene: Metathesis Polymerization, Degradation, and Reformation

Kyoungwon Lee, Hong-Gyu Seong, Thomas P. Russell, and Todd Emrick*

Cite This: ACS Macro Lett. 2025, 14, 616−621 Read Online

ACCESS | Metrics & More | Article Recommendations | Supporting Information

ABSTRACT: The enormous global production and use of polymers and plastics, combined with slower and less efficient disposal and recycling methods, have led to a worldwide growth in plastic waste. Here, we describe an approach that builds degradability into macromolecular polyolefins through the design of telechelic oligomers with reactive functional groups that enables control over polymer deconstruction and reconstruction. Our work exploits disulfide-containing polymers that have emerged as promising cyclable materials due to their dynamic reversibility (bond formation and cleavage) driven by redox chemistry under mild conditions. Specifically, we describe the synthesis of a telechelic α,ω-dithiopolycyclooctene (PCOE) by ring-opening metathesis polymerization using a dithioacetate chain transfer agent, followed by deprotection to convert the chain-end thioacetates to thiols. This process was studied towards control over the degree of oxidation to yield disulfide-containing PCOE, followed by an evaluation of reductive degradation and oxidative repolymerization. Overall, this approach facilitates the production of disulfide-containing unsaturated polyolefins and the integration of degradable and reformable moieties into soluble, processable, metathesis-derived polymers.

The remarkable advances enabled by synthetic polymers have resulted in their extensive incorporation across nearly all aspects of society.[1−4] Polyolefins, in particular, represent a major percentage of the volume of all plastics produced for essential products of daily life, due to their ease of processability and excellent mechanical and thermal properties.[5−9] However, the intrinsic properties of polyolefins include their slow degradation (i.e., molecular weight reduction), which has led to their environmental accumulation, disposal in landfills, or generation of emissions associated with incineration.[10,11] Therefore, recycling and upcycling efforts focused largely on polyolefins are often conducted by mechanical or chemical approaches. However, the products obtained from conventional mechanical recycling tend to exhibit diminished properties relative to pristine materials, in many cases due to loss of homogeneity in the recycled product.[12−14] In chemical recycling, molecular-level polymer deconstruction is needed to recapture pristine polymer products, i.e., in a closed-loop cycle.[14−16] As would be anticipated, a complete deconstruction from polymer to monomer is required to optimize the purity and properties of the newly synthesized polymer, but achieving this requires efficient reactions with extensive energy consumption and therefore cost.[17]

To balance the advantages and drawbacks of chemical recycling and circumvent the need to recover pure monomers, polymer deconstruction to oligomeric molecules represents a rational and potentially simpler approach.[18,19] For polyolefins, one such strategy uses telechelic oligomers with reactive functional groups. For instance, α,ω-difunctional polyolefins are synthesized efficiently using α,ω-substituted chain transfer agents (CTAs) with cyclic olefins, generally cyclooctene (COE), and ruthenium benzylidene-catalyzed ring-opening metathesis polymerization (ROMP).[20−22] In this mechanism, ROMP of COE is the fast step in the process and is terminated by cross metathesis (CM) reactions with the CTA to yield the end-functionalized polymer products with excellent chain-end fidelity, where the [COE]:[CTA] ratio at fixed catalyst amount dictates the molecular weight of the polymer product.[23] For example, Hillmyer and co-workers used ROMP to prepare carboxylic acid−terminated telechelic poly(cyclooctene) (PCOE) from COE and maleic acid[24] as well as hydroxyl-terminated telechelic polyolefins using COE in combination with *cis*-7-hexadecene-1,16-diol as the CTA.[25] In further work, Miyake and co-workers utilized hydroxyl-terminated telechelic polyolefins derived by ROMP in conjunction with a ruthenium complex and $H_{2(g)}$ as catalyst in reversible polyester formation/degradation.[26] These and other examples reviewed recently reflect the trade-offs of synthetic methods and energy consumption associated with macromolecular construction and deconstruction.[27]

Received: April 13, 2025
Revised: April 17, 2025
Accepted: April 18, 2025
Published: May 2, 2025

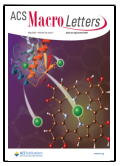

https://doi.org/10.1021/acsmacrolett.5c00245
ACS Macro Lett. 2025, 14, 616−621

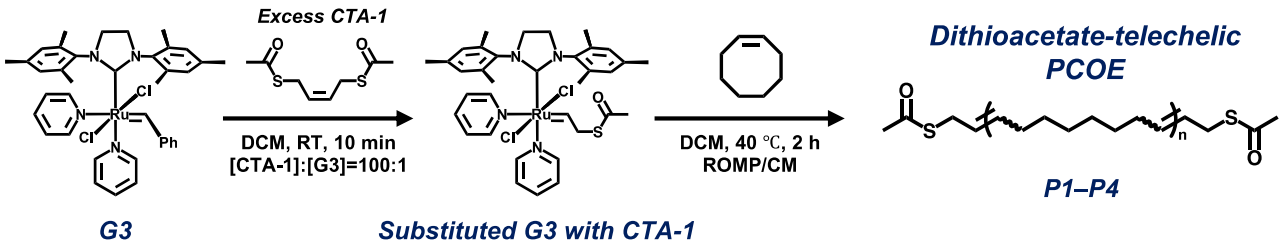

Figure 1. Synthesis of telechelic dithioacetate-terminated PCOE using ROMP of COE in the presence of **CTA-1** and the **G3** ruthenium benzylidene metathesis catalyst.

Table 1. Summary of Results for the Preparation of P1−P4 by ROMP of COE with CTA-1

Entry[a]	[COE]:[CTA-1]:[G3]	Target DP	$M_{n,theo}$ (kDa)	$M_{n,NMR}$[b] (kDa)	DP[b]	$M_{n,SEC}$[c] (kDa)	$Đ$[c]	% Yield[d]
P1	1000:100:1	10	1.2	1.9	16	3.3	1.61	97
P2	2000:100:1	20	2.4	3.5	30	6.2	1.69	94
P3	5000:100:1	50	6.0	6.7	59	12.2	1.76	97
P4	10000:100:1	100	11.2	9.3	83	18.6	1.63	96

[a]Conditions: all entries used 15.4 mmol of COE and reaction times of 2 h in refluxing DCM. [b]Determined by ^{1}H NMR spectroscopy. [c]Estimated by SEC, with THF as the mobile phase and polystyrene calibration standards. [d]Determined gravimetrically following polymer isolation by precipitation.

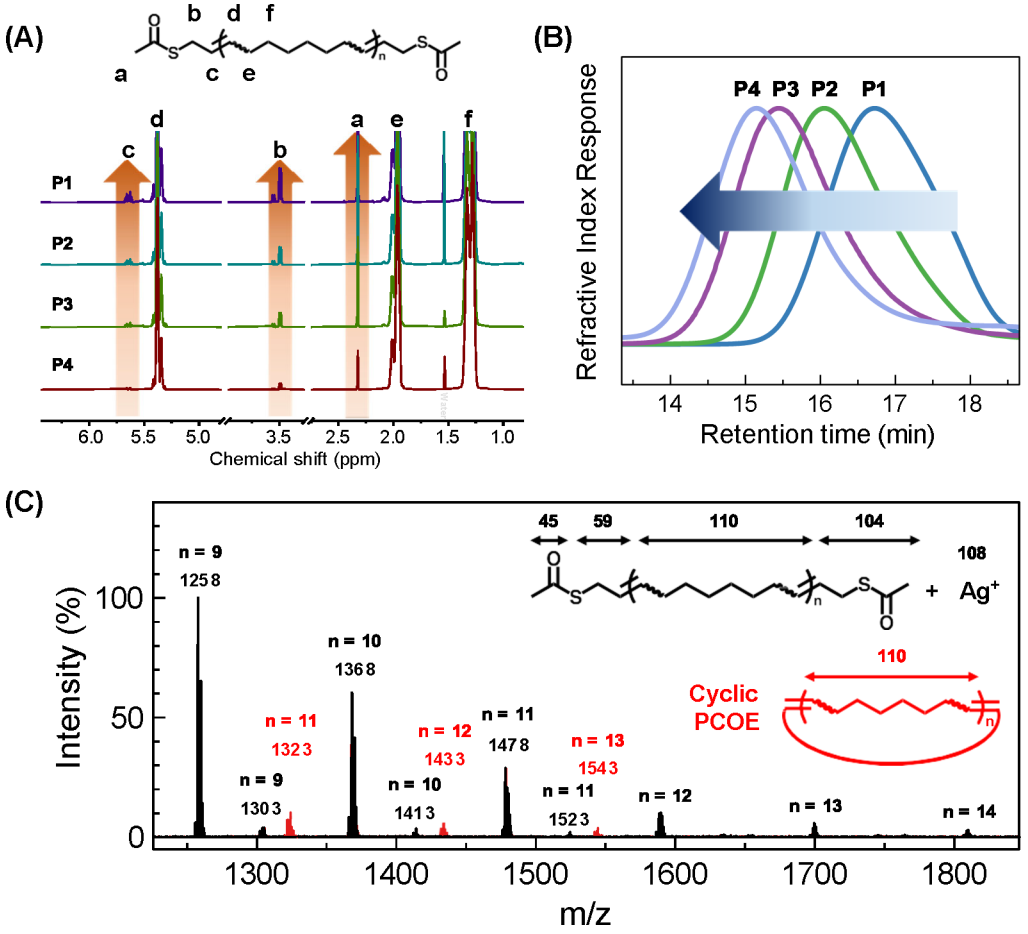

Figure 2. (A) ^{1}H NMR spectra and (B) SEC traces of **P1−P4**. (C) MALDI-ToF mass spectrum of **P1**.

To enhance their chemical stability and recyclability, we are interested in new methods that effectively build polyolefins containing internal disulfides and chain-end thiols. Examples of prior work in our group showed that disulfide-containing cyclic olefins capably undergo ROMP, including an 8-membered ring that was copolymerized with COE[28] and a 6-membered ring that was prepared, prepared in one step by ring-closing metathesis of the commercial diallyl disulfide.[29] Both approaches effectively insert disulfide units into unsaturated polyolefins by using metathesis chemistry. In an alternative approach, the utility of alternating diene metathesis polymerization was demonstrated with disulfide-containing α,ω-

https://doi.org/10.1021/acsmacrolett.5c00245
ACS Macro Lett. 2025, 14, 616−621

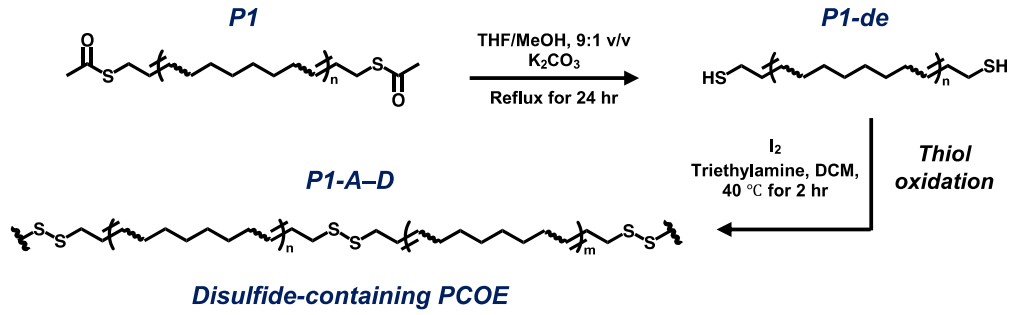

Figure 3. Deprotection of **P1**, followed by oxidative polymerization, to yield disulfide-containing PCOE (**P1-A–D**).

diacrylates and 1,9-decadiene, affording alternating copolymers having low-to-modest degree-of-polymerization (DP) values.[30]

As illustrated in Figure 1, in this paper is described the preparation of disulfide-containing polyolefins by performing ROMP of COE in the presence of the CTA *cis*-2-butene-1,4-dithioacetate (**CTA-1**) with a Grubbs third-generation metathesis catalyst (**G3**). This yielded dithioacetate–telechelic PCOEs **P1–P4** using **CTA-1** that were converted easily to α,ω-dithiol versions, which are set up for oxidative polymerization under mild conditions. Each step of the process was characterized by NMR spectroscopy and size exclusion chromatography (SEC) to reveal both compositional and molecular weight control. To our knowledge, this is the first use of an α,ω-dithioacetate CTA in metathesis polymerization, the successful implementation of which paves the way for new approaches to recyclable or upcyclable polyolefins.

Exploiting the reversibility of thiol/disulfide chemistry in polyolefins required starting from polymeric α,ω-dithiols that were synthesized in two steps: 1) ROMP of COE in the presence of **CTA-1** and 2) thioacetate deprotection to yield the dithiol–telechelic PCOE (dithiol-PCOE). **CTA-1** was synthesized from *cis*-1,4-dichloro-2-butene and potassium thioacetate[31] and characterized by NMR spectroscopy (Figure S1). To test the compatibility of **CTA-1** with ruthenium benzylidene catalyst **G3**, *in situ* solution ($CDCl_3$) NMR analysis was performed at **CTA-1**:**G3** molar ratios of 10:1 and 100:1 ([**G3**] ≃ 20 mM) (Supporting Information). Initially, the benzylidene proton resonance of **G3** was seen as a singlet at 19.18 ppm; however, over time, the benzylidene signal intensity decreased in favor of a triplet centered at 18.29 ppm, representing the resonances of new ruthenium alkylidenes substituted with **CTA-1** (Figure S2). At both molar ratios, full and fast conversion to product (in minutes) was observed, noting that reactions performed at higher **CTA**:**G3** ratios proceeded more quickly. Based on *in situ* NMR experiments, **CTA-1** was found to be compatible with the metathesis catalyst. ROMP reactions using COE, **CTA-1**, and **G3** were then performed in refluxing DCM by setting the COE concentration to 2.0 M and varying the [**COE**]:[**CTA-1**] ratios to set the targeted DP values of **P1–P4**, fixing the **CTA-1**:**G3** molar ratio at 100:1 in order to minimize the production of chains terminated with thiol at only one end. The PCOE products were isolated as off-white powders in excellent yield (>90%) after precipitation into cold MeOH, with a summary of ROMP results and molecular weight characterization summarized in Table 1.

NMR spectroscopy and SEC characterization confirmed the successful synthesis of the desired telechelic PCOE structures. As shown in Figures 2A (**P1–P4** ^{1}H NMR spectra) and S3 (^{1}H–^{1}H COSY and ^{1}H–^{13}C HSQC NMR spectra of **P1**), distinct ^{1}H NMR resonances, such as the thioacetate methyl group (2.32 ppm, $C\underline{H}_3$–$C(O)S$-CH_2-) and neighboring methylene groups (d, 3.5 ppm, –S-$C\underline{H}_2$-CH=CH–), enabled determination of M_n by end-group analysis (Figure S4A), giving values in the 1–9 kDa range that correlated closely with targeted values. Further NMR analysis showed the dominance of *trans* olefins (≥78%) in the PCOE backbone, whereas the chain-end connection with **CTA-1** is predominantly *cis* (≥84%) (Figure S4B). SEC-estimated molecular weights ranged from 3 to 18 kDa (dispersity ($Đ$) ∼ 1.7), as analyzed by eluting in THF against polystyrene calibration standards; the elution profiles shifted to shorter retention time (i.e., higher molecular weight) at higher **COE**:**CTA-1** molar ratios (Figure 2B). FT-IR spectroscopy confirmed the presence of thioacetate in the polymer products from the characteristic C=O stretching (1694 cm^{-1}) (Figure S4C). MALDI-ToF analysis of **P1** (Figure 2C) showed the dominant molecular weight population to align well with values derived from both $M_{n,theo}$ and $M_{n,NMR}$ at a COE repeat unit of 110 g mol^{-1}. For example, for n = 9, the major signal corresponds to m/z_{calc} = 1258 g mol^{-1} $[M–CH_3CO]^+$, representing the mass fragment of telechelic polymer with loss of an acetyl chain-end, while the minor population without fragmentation appears at 1303 g mol^{-1}. Small but discernible signals were observed at m/z_{calc} of 1323, 1433, and 1543 g mol^{-1} for n = 11, 12, and 13, respectively, which correspond to cyclic PCOE structures that likely arise from the relatively high concentrations employed in these polymerizations.[21,32]

The successful outcomes of metathesis polymerizations performed in the presence of the thioacetate-functionalized CTA were found to contrast similar experiments using CTAs containing thiol or disulfide groups, which are typically problematic in metathesis polymerization.[28–30,33,34] For example, attempted ROMP of COE in the presence of α,ω-dithiol **CTA-2** (prepared from **CTA-1** with K_2CO_3 in MeOH (Figure S5)) by the same procedure as for **CTA-1** (i.e., **CTA**:**G3** (100:1)) was unsuccessful owing to catalyst decomposition, as confirmed by *in situ* ^{1}H NMR spectroscopy in $CDCl_3$. At 10:1 CTA:G3, high metathesis conversion (i.e., substitution of **G3** with **CTA-2**) was achieved, with the expected appearance of a new ruthenium alkylidene signal at 17.02 ppm (Figure S6); however, productive ROMP did not occur (Table S1) (Supporting Information).

Thioacetate deprotection was conducted as an alternative approach to afford α,ω-dithiol-PCOE. In the design illustrated in Figure 3, using **P1** as a representative example, deprotection under basic conditions produced the desired dithiol-PCOE (**P1-de**), which was followed by oxidative disulfide formation to afford the corresponding PCOE polymers (**P1-A–D**).

https://doi.org/10.1021/acsmacrolett.5c00245
ACS Macro Lett. 2025, 14, 616–621

Specifically, thioacetate deprotection was performed in THF/MeOH (9:1 v/v) using excess K_2CO_3 in refluxing THF to afford **P1-de** as an off-white powder in high yield (≥90%) after precipitation into cold MeOH. In the ^{1}H NMR spectrum of the deprotected product (Figure S7A), the methyl proton resonance from the thioacetate precursor (2.32 ppm, $C\underline{H}_3{-}C(O)S{-}CH_2{-}$) was notably absent, and the resonance for the methylene protons adjacent to the thioacetate of **P1** (d, 3.5 ppm, $-(O)C\ S{-}C\underline{H}_2{-}CH{=}CH{-}$) shifted to 3.13 ppm (m) in **P1-de**, indicative of conversion to the thiol ($HS{-}C\underline{H}_2{-}CH{=}CH{-}$). A distinct triplet for the thiol appeared at 1.39 ppm ($\underline{H}S{-}CH_2{-}CH{=}CH{-}$). ^{13}C NMR further confirmed loss of the thioacetate carbonyl (195 ppm, $CH_3{-}\underline{C}(O)S{-}CH_2{-}$) (Figure S7B), as did FT-IR spectroscopy with the characteristic C=O stretching signal absent (Figure S8A). To augment this spectroscopic data, molecular weight characterization by MALDI-ToF showed the major population of **P1-de** to have the expected COE repeat unit (110 g mol^{-1}) and the mass fragments corresponding to the α,ω-dithiol. For example, the n = 10 mass fragment, $m/z_{\ calc}$ = 1295 g mol^{-1}, corresponds to loss of one chain-end thiol $[M{-}SH]^+$ (Figure S8C). In addition, as for **P1**, a small population of cyclic PCOE was also observed with $m/z_{\ calc}$ = 1323, 1433, and 1543 g mol^{-1} for n = 11, 12, and 13, respectively. As expected, the telechelic dithiol **P1-de** underwent some degree of oxidation upon workup and storage: ^{1}H NMR spectroscopy indicated about 7% oxidation by integration of the methylene protons adjacent to thiol ($HS{-}C\underline{H}_2{-}CH{=}CH{-}$) signals at 3.13 ppm (m) vs the methylene protons adjacent to disulfide ($-C\underline{H}_2{-}SS{-}C\underline{H}_2{-}$) at 3.29 ppm (d) (Figure S9). This minor degree of oxidation led to only a small molecular weight increase by SEC, from 3.3 kDa for the thioacetate precursor to 3.5 kDa for the disulfide (Figure S8B).

For oxidative polymerization of the telechelic dithiol-PCOE (**P1-de**), the degree of oxidation was controlled by adjusting the thiol-to-oxidant stoichiometry using iodine/triethylamine in refluxing DCM as the oxidative environment. This yielded disulfide-containing PCOE (**P1-A–D**) in which the relative ratio of chain-end thiols vs in-chain disulfides was calculated by ^{1}H NMR spectroscopy (Supporting Information). The results in Table 2, entries **P1-A** to **P1-D**, were obtained using 0.05 mmol of **P1-de** with varying amounts of oxidant, showing that disulfide bond formation resulted in a substantial increase in molecular weight (M_w range from 5.5 up to 26.8 kDa). With increasing conversion, NMR resonances from the thiol chain ends (t, 1.39 ppm, $\underline{H}S{-}CH_2{-}CH{=}CH{-}$) decreased significantly, and methylene protons adjacent to the thiol/disulfide bond showed decrement/increment (Figure S9), respectively. Conveniently, the dithiol-to-oxidant ratio afforded control over the molecular weight of the polymer product. For example, in Table 2, entries **P1-D**, **P1-D1**, and **P1-D2** aimed for complete oxidation via the use of excess oxidant, which was confirmed spectroscopically (Figure S9). **P1-D1** and **P1-D2** used 0.1 and 0.2 mmol of **P1-de**, respectively, resulting in molecular weight increases that were proportional to the amount of original thiol, and confirmed by SEC showing **P1-D1** (M_w = 35.0 kDa) and **P1-D2** (M_w = 44.3 kDa). Regardless of polymerization conditions, the polymer products showed high $Đ$ values (up to 5) relative to conventional A–A step-growth polymerization, due at least in part to the presence of a residual cyclic polymer. Indeed, cyclization was confirmed by MALDI-TOF analysis (Figure 2(C) and Figure S8), while SEC showed a signal reflecting low molecular weight polymer ($M_p \simeq$ 2.4 kDa, ∼17 min retention time) after this oxidative polymerization (Figure S10).

Incorporating disulfide bonds into the PCOE backbone enabled degradation under reducing conditions; complete degradation would afford the original α,ω-dithiol-PCOE. As illustrated in Figure 4A, the dynamic characteristics of the disulfide units were demonstrated with **P1-D2**, initially by formation of high molecular weight material associated with efficient oxidation (M_w = 44.3 kDa). Disulfide reduction was conducted using n-Bu_3P in refluxing DCM for 1 h, yielding **P1-D2-R1** (1st reduction cycle product, M_w = 5.8 kDa) and isolation of an off-white powder in 89% yield after precipitation into cold MeOH. SEC showed that the molar mass distribution of **P1-D2-R1** corresponded closely with that of **P1-de**. A second oxidation cycle was then performed to yield **P1-D2-O2** (M_w = 42.8 kDa), nearly reaching the original molar mass of **P1-D2** (Supporting Information). The second

Table 2. Summary of Oxidation Reaction with P1-de

Entry[a]	Oxidation[c] (%)	M_w[d] (kDa)	PDI[d]	Yield[e] (%)
P1-de	7	5.5	1.59	90
P1-A	23	6.6	1.50	89
P1-B	45	10.5	2.12	96
P1-C	95	26.8	5.14	81
P1-D	>99	25.2	5.29	91
P1-D1[b]	>99	35.0	3.56	92
P1-D2[b]	>99	44.3	4.73	89

[a]Conditions: **P1-A–P1-D** entries used **P1-de** (0.05 mmol), varying amounts of iodine, and a reaction time of 2 h in refluxing DCM. [b]**P1-D1** and **P1-D2** entries targeted complete oxidation and used 0.1 and 0.2 mmol of **P1-de**, respectively. [c]Determined by ^{1}H NMR spectroscopy. [d]Estimated by SEC, with THF as eluent, and polystyrene calibration standards. [e]Determined gravimetrically after isolation of polymer by precipitation into MeOH.

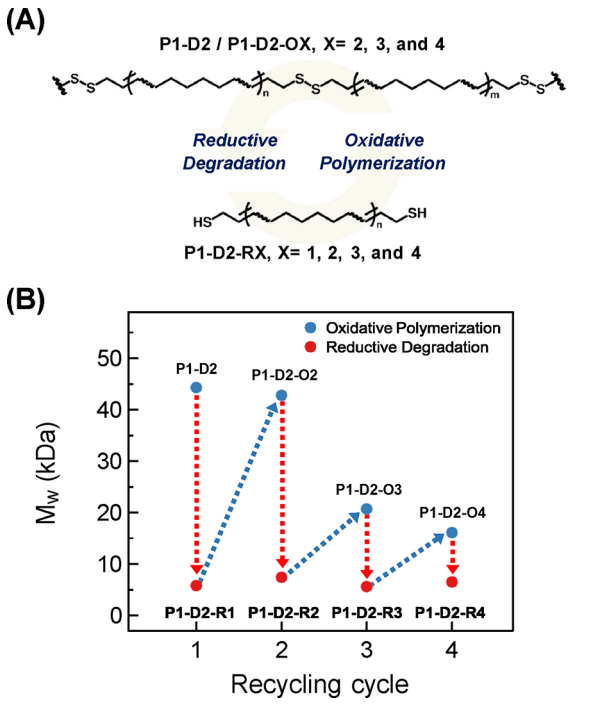

Figure 4. (A) Schematic representation of thiol–disulfide cycling and (B) molecular weight results for each step of the cycling process.

https://doi.org/10.1021/acsmacrolett.5c00245
ACS Macro Lett. 2025, 14, 616–621

reduction was conducted with **P1-D2-O2** to afford **P1-D2-R2** (M_w = 7.4 kDa). Figure 4B and Table 3 summarize the results

Table 3. Summary of P1-D2 Cycling

Entry	Oxidation[b] (%)	M_w[c] (kDa)	$Đ$[c]	Yield[d] (%)
P1-D2	>99	44.3	4.73	89
P1-D2-R1	7	5.8	1.46	89
P1-D2-O2[a]	>99	42.8	4.28	87
P1-D2-R2	10	7.4	1.79	78
P1-D2-O3[a]	96	20.7	4.21	76
P1-D2-R3	14	5.6	1.70	81
P1-D2-O4[a]	97	16.1	3.95	79
P1-D2-R4	31	6.5	1.66	77

[a]The same molar amount (0.2 mmol, same as **P1-D2** entry) is used for the oxidative polymerization, and the deficient amount of the thiol group after the purification step from the reduction step (**P1-D2-R*X***, ***X*** = **2** and **3**) is supplemented with **P1-de**. [b]Determined by ^{1}H NMR spectroscopy. [c]Estimated by SEC, with THF as the eluent, calibrated with polystyrene standards. [d]Determined gravimetrically following isolation of polymer by precipitation into cold MeOH.

of four cycles, showing that in the third and fourth cycles the molecular weights of the oxidized product reached 20.7 and 16.1 kDa, respectively. The polymer molecular weight distribution and structures at each step were measured by SEC (Figure S11) and ^{1}H NMR spectroscopy (Figure S12A), where key NMR confirmed cyclability from the intensity of the methylene proton signals adjacent to the disulfide bonds (d, 3.29 ppm, $-C\underline{H}_2-SS-C\underline{H}_2-$) and those adjacent to thiol (m, 3.13 ppm, $HS-C\underline{H}_2-CH{=}{=}CH-$). The efficiency of the process declined in later cycles, reaching ∼40 kDa in the second cycle and only 16 kDa in the fourth cycle, whereas the molecular weights of the reduction cycle products (**P1-D2-R*X***, **X** = **1**−**4**) were similar. ^{1}H NMR spectroscopy of the reduced polymers suggested a loss of some percentage of the needed thiol chain-end in the later cycles (Figure S12B). Such impacts of even relatively minor side reactions on molecular weights of successive cycles are expected, seen for example in reports of Bates and co-workers on thiol-based polymers prepared from acrylates and α-lipoic acid.[35] Notably, the ability to perform thiol/disulfide cycling in the absence of cross-linking, such as through undesired thiol−ene reactions, bodes well for extension of these cycling reactions to a range of unsaturated cyclic olefins and related structures.

In summary, telechelic dithioacetate−PCOEs were synthesized successfully using ROMP with **CTA-1**, resulting in a range of molecular weights (i.e., from 1 to 9 kDa). MALDI-ToF analysis supported the telechelic structure of PCOE, with the major molecular weight populations corresponding closely to the theoretical values. Thioacetate deprotection afforded dithiol-PCOE, which enabled subsequent molecular weight recovery and degradation *via* redox chemistry. Using **P1-de** (dithiol-PCOE, 5.5 kDa) as the starting material, oxidation produced disulfide-containing PCOE up to considerable molecular weight values (>40 kDa), tailored by adjusting the degree of oxidation and the stoichiometry of thiol and oxidant. These disulfide-containing polymers gave access to cyclability, with the effectiveness of each step monitored spectroscopically and chromatographically. Overall, this synthetic route highlights a promising methodology for cycling the molecular weight of polyolefins, offering a foundation for further research in sustainable polymer design and strategic circularity, in which designs in macromolecular breakdown, recovery, and buildup are beneficial.

■ ASSOCIATED CONTENT

Supporting Information

The Supporting Information is available free of charge at https://pubs.acs.org/doi/10.1021/acsmacrolett.5c00245.

Experimental procedures for synthesis of chain-transfer agents and polymers; methods and experimental setup for characterization using the following methods: NMR, FT-IR, SEC, and MALDI-ToF; kinetics studies and characterization of polymer cycling (PDF)

■ AUTHOR INFORMATION

Corresponding Author

Todd Emrick − *Polymer Science & Engineering Department, Conte Center for Polymer Research, University of Massachusetts, Amherst, Massachusetts 01003, United States;* orcid.org/0000-0003-0460-1797; Email: tsemrick@mail.pse.umass.edu

Authors

Kyoungwon Lee − *Polymer Science & Engineering Department, Conte Center for Polymer Research, University of Massachusetts, Amherst, Massachusetts 01003, United States*

Hong-Gyu Seong − *Polymer Science & Engineering Department, Conte Center for Polymer Research, University of Massachusetts, Amherst, Massachusetts 01003, United States*

Thomas P. Russell − *Polymer Science & Engineering Department, Conte Center for Polymer Research, University of Massachusetts, Amherst, Massachusetts 01003, United States; Materials Sciences Division, Lawrence Berkeley National Laboratory, Berkeley, California 94720, United States;* orcid.org/0000-0001-6384-5826

Complete contact information is available at: https://pubs.acs.org/10.1021/acsmacrolett.5c00245

Notes

The authors declare no competing financial interest.

■ ACKNOWLEDGMENTS

T.E. acknowledges support of this research from the Donors of the American Chemical Society Petroleum Research Fund (PRF, #68011-ND7), as well as Agilent Technologies for the 1260 Infinity II SEC-MALS system, and T.P.R. acknowledges support from the Army Research Office under contract W911NF-24-2-0041.

■ REFERENCES

(1) Huang, Z. M.; Zhang, Y. Z.; Kotaki, M.; Ramakrishna, S. A Review on Polymer Nanofibers by Electrospinning and Their Applications in Nanocomposites. *Compos. Sci. Technol.* **2003**, *63*, 2223−2253.

(2) Ding, L.; Yu, Z. Di; Wang, X. Y.; Yao, Z. F.; Lu, Y.; Yang, C. Y.; Wang, J. Y.; Pei, J. Polymer Semiconductors: Synthesis, Processing, and Applications. *Chem. Rev.* **2023**, *123*, 7421−7497.

(3) Li, G.; Zhu, R.; Yang, Y. Polymer Solar Cells. *Nat. Photonics* **2012**, *6*, 153−161.

(4) Pack, D. W.; Hoffman, A. S.; Pun, S.; Stayton, P. S. Design and Development of Polymers for Gene Delivery. *Nat. Rev. Drug Discovery* **2005**, *4*, 581−593.

(5) Zanchin, G.; Leone, G. Polyolefin Thermoplastic Elastomers from Polymerization Catalysis: Advantages, Pitfalls and Future Challenges. *Prog. Polym. Sci.* **2021**, *113*, No. 101342.
(6) Chodák, I. Properties of Crosslinked Polyolefin-Based Materials. *Prog. Polym. Sci.* **1995**, *20* (6), 1165−1199.
(7) Galli, P.; Vecellio, G. Polyolefins: The Most Promising Large-Volume Materials for the 21st Century. *J. Polym. Sci., Part A: Polym. Chem.* **2004**, *42*, 396−415.
(8) Khanam, P. N.; AlMaadeed, M. A. A. Processing and Characterization of Polyethylene-Based Composites. *Advanced Manufacturing: Polymer and Composites Science* **2015**, *1*, 63−79.
(9) Mohite, A. S.; Rajpurkar, Y. D.; More, A. P. Bridging the Gap between Rubbers and Plastics: A Review on Thermoplastic Polyolefin Elastomers. *Polym. Bull.* **2022**, *79*, 1309−1343.
(10) Hahladakis, J. N.; Velis, C. A.; Weber, R.; Iacovidou, E.; Purnell, P. An Overview of Chemical Additives Present in Plastics: Migration, Release, Fate and Environmental Impact during Their Use, Disposal and Recycling. *J. Hazard. Mater.* **2018**, *344*, 179−199.
(11) Geyer, R.; Jambeck, J. R.; Law, K. L. Production, Use, and Fate of All Plastics Ever Made. *Science Advances* **2017**, *3*, No. e1700782.
(12) Ignatyev, I. A.; Thielemans, W.; Vander Beke, B. Recycling of Polymers: A Review. *ChemSusChem* **2014**, *7*, 1579−1593.
(13) Ragaert, K.; Delva, L.; Van Geem, K. Mechanical and Chemical Recycling of Solid Plastic Waste. *Waste Management* **2017**, *69*, 24−58.
(14) Westlie, A. H.; Chen, E. Y. X.; Holland, C. M.; Stahl, S. S.; Doyle, M.; Trenor, S. R.; Knauer, K. M. Polyolefin Innovations toward Circularity and Sustainable Alternatives. *Macromol. Rapid Commun.* **2022**, *43* (24), 2200492.
(15) Epps, T. H., III; Korley, L. T.; Yan, T.; Beers, K. L.; Burt, T. M. Sustainability of Synthetic Plastics: Considerations in Materials Life-Cycle Management. *JACS Au* **2022**, *2* (1), 3−11.
(16) Tan, Y.; Cheng, Y.; Xu, J.; Wang, H. Catalytic Chemical Recycling and Upcycling of Polyolefin Plastics. *Giant* **2024**, *19*, No. 100307.
(17) Schwab, S. T.; Baur, M.; Nelson, T. F.; Mecking, S. Synthesis and Deconstruction of Polyethylene-Type Materials. *Chem. Rev.* **2024**, *124*, 2327−2351.
(18) Geyer, B.; Röhner, S.; Lorenz, G.; Kandelbauer, A. Designing Oligomeric Ethylene Terephtalate Building Blocks by Chemical Recycling of Polyethylene Terephtalate. *J. Appl. Polym. Sci.* **2014**, *131*, 39786.
(19) Ng, K. W. J.; Lim, J. S. K.; Gupta, N.; Dong, B. X.; Hu, C. P.; Hu, J.; Hu, X. M. A Facile Alternative Strategy of Upcycling Mixed Plastic Waste into Vitrimers. *Communications Chemistry* **2023**, *6* (1), 158.
(20) Morita, T.; Maughon, B. R.; Bielawski, C. W.; Grubbs, R. H. Ring-Opening Metathesis Polymerization (ROMP) Approach to Carboxyl- and Amino-Terminated Telechelic Poly(Butadiene)s. *Macromolecules* **2000**, *33* (17), 6621−6623.
(21) Vanbiervliet, E.; Fouquay, S.; Michaud, G.; Simon, F.; Carpentier, J. F.; Guillaume, S. M. From Epoxide to Cyclo-dithiocarbonate Telechelic Polycyclooctene through Chain-Transfer Ring-Opening Metathesis Polymerization (ROMP): Precursors to Non-Isocyanate Polyurethanes (NIPUS). *Macromolecules* **2017**, *50* (1), 69−82.
(22) Pal, S.; Alizadeh, M.; Kilbinger, A. F. M. Telechelics Based on Catalytic Alternating Ring-Opening Metathesis Polymerization. *ACS Macro Lett.* **2019**, *8* (10), 1396−1401.
(23) Yan, T.; Guironnet, D. Synthesis of Telechelic Polyolefins. *Polym. Chem.* **2021**, *12*, 5126−5138.
(24) Pitet, L. M.; Hillmyer, M. A. Carboxy-Telechelic Polyolefins by ROMP Using Maleic Acid as a Chain Transfer Agent. *Macromolecules* **2011**, *44* (7), 2378−2381.
(25) Sample, C. S.; Kellstedt, E. A.; Hillmyer, M. A. Tandem ROMP/Hydrogenation Approach to Hydroxy-Telechelic Linear Polyethylene. *ACS Macro Lett.* **2022**, *11* (5), 608−614.
(26) Zhao, Y.; Rettner, E. M.; Harry, K. L.; Hu, Z.; Miscall, J.; Rorrer, N. A.; Miyake, G. M. Chemically Recyclable Polyolefin-like Multiblock Polymers. *Science* **2023**, *382*, 310−314.
(27) Sun, H.; Liang, Y.; Thompson, M. P.; Gianneschi, N. C. Degradable Polymers via Olefin Metathesis Polymerization. *Prog. Polym. Sci.* **2021**, *120*, No. 101427.
(28) Chang, C. C.; Emrick, T. Functional Polyolefins Containing Disulfide and Phosphoester Groups: Synthesis and Orthogonal Degradation. *Macromolecules* **2014**, *47* (4), 1344−1350.
(29) Seong, H. G.; Russell, T. P.; Emrick, T. Degradable Polyolefins Prepared by Integration of Disulfides into Metathesis Polymerizations with 3,6-Dihydro-1,2-Dithiine. *Chemical Science* **2024**, *15*, 17084−17091.
(30) Lee, K.; Russell, T. P.; Emrick, T. Impacts of Disulfide-Containing Monomers in Alternating Diene Metathesis Polymerization. *J. Polym. Sci.* **2025**, *63*, 678.
(31) Kato, T.; Lim, B.; Cheng, Y.; Pham, A. T.; Maynard, J.; Moreau, D.; Poblador-Bahamonde, A. I.; Sakai, N.; Matile, S. Cyclic Thiosulfonates for Thiol-Mediated Uptake: Cascade Exchangers, Transporters, Inhibitors. *JACS Au* **2022**, *2* (4), 839−852.
(32) Michel, X.; Fouquay, S.; Michaud, G.; Simon, F.; Brusson, J. M.; Carpentier, J. F.; Guillaume, S. M. α,ω-Bis(Trialkoxysilyl) Difunctionalized Polycyclooctenes from Ruthenium-Catalyzed Chain-Transfer Ring-Opening Metathesis Polymerization. *Polym. Chem.* **2016**, *7* (29), 4810−4823.
(33) Wagener, K. B.; Brzezinska, K.; Anderson, J. D.; Younkin, T. R.; Steppe, K.; DeBoer, W. Kinetics of Acyclic Diene Metathesis (ADMET) Polymerization. Influence of the Negative Neighboring Group Effect. *Macromolecules* **1997**, *30*, 7363−7369.
(34) Hillmyer, M. A.; Nguyen, S. T.; Grubbs, R. H. Utility of a Ruthenium Metathesis Catalyst for the Preparation of End-Functionalized Polybutadiene. *Macromolecules* **1997**, *30* (4), 718−721.
(35) Albanese, K. R.; Okayama, Y.; Morris, P. T.; Gerst, M.; Gupta, R.; Speros, J. C.; Hawker, C. J.; Choi, C.; De Alaniz, J. R.; Bates, C. M. Building Tunable Degradation into High-Performance Poly(Acrylate) Pressure-Sensitive Adhesives. *ACS Macro Lett.* **2023**, *12* (6), 787−793.

https://doi.org/10.1021/acsmacrolett.5c00245
ACS Macro Lett. 2025, 14, 616−621